Canadian Geotechnical Journal

OPEN ACCESS | Research Article

Experimental and numerical evaluation of the potential reuse of waste rock as an evaporation barrier in engineered cover systems: effects of particle size

Karine Sylvain[a], **Isabelle Demers**[a], **and Thomas Pabst**[b]

[a]Research Institute on Mines and Environment (RIME) UQAT-Polytechnique, Université du Québec en Abitibi-Témiscamingue, Rouyn-Noranda, QB, Canada; [b]Norwegian Geotechnical Institute (NGI), Oslo, Norway

Corresponding author: **Karine Sylvain** (email: karine.sylvain@uqat.ca)

Abstract

One of the key challenges for the mining industry is the development of effective and durable management, closure, and reclamation strategies for acid mine drainage (AMD) generating tailings storage facilities (TSF). The elevated water table technique is particularly effective in preventing AMD under humid and temperate climate, as it reduces oxygen fluxes by maintaining the tailings saturated. A protection layer made of coarse-grained material (capillary break) is often needed to enhance water infiltration and reduce evaporation by reducing capillaries upward flow. A sustainable approach therefore consists in reusing waste rock to build this layer, reducing surface-stored mine waste and the environmental impact of borrow pits. However, the heterogeneity and reactivity of waste rock have so far limited their large-scale valorization in cover systems. The objective of this research was to evaluate the potential reuse of different size fractions of waste rock in an evaporation barrier. Laboratory column tests were carried out to evaluate the effectiveness of the cover made of waste rock to control water balance. Results indicated that waste rock containing fine fractions were less efficient in reducing evaporation than coarser fractions without fines for shallow water table. Numerical simulations were also carried out successfully to reproduce the effect of particle size on evaporation fluxes. This study underlines the importance of optimizing the particle size distribution in the design of evaporation barriers.

Key words: waste rock valorization, circular economy, evaporation, integrated waste management, mine waste reclamation

Résumé

L'un des principaux défis pour l'industrie minière est l'élaboration de stratégies efficaces et durables de gestion, de fermeture et de remise en état des installations de stockage de résidus miniers (TSF), susceptibles de générer du drainage minier acide (DMA). La technique de la nappe phréatique élevée est particulièrement efficace pour prévenir le DMA dans les climats humides et tempérés, car elle réduit les flux d'oxygène en maintenant les résidus saturés. Une couche de protection faite d'un matériau à gros grains (jouant un rôle de rupture capillaire) est souvent nécessaire pour favoriser l'infiltration de l'eau et réduire l'évaporation en limitant l'écoulement capillaire ascendant. Une approche durable consiste donc à réutiliser les stériles pour construire cette couche, réduisant ainsi les résidus miniers entreposés en surface et l'impact environnemental des fosses d'emprunt. Cependant, l'hétérogénéité et la réactivité des stériles ont jusqu'à présent limité leur valorisation à grande échelle dans les systèmes de recouvrement. L'objectif de cette recherche était d'évaluer la réutilisation potentielle de fractions de différentes tailles de stériles dans une barrière d'évaporation. Des essais sur colonne en laboratoire ont été réalisés pour évaluer l'efficacité de la couverture faite de stériles pour contrôler le bilan hydrique. Les résultats ont indiqué que les stériles contenant des fractions fines étaient moins efficaces pour réduire l'évaporation que les fractions plus grossières sans fines, dans le cas d'une nappe phréatique peu profonde. Des simulations numériques ont également été réalisées avec succès pour reproduire l'effet de la taille des particules sur les flux d'évaporation. Cette étude souligne l'importance d'optimiser la distribution granulométrique dans la conception des barrières d'évaporation.

Mots-clés : valorisation des stériles, économie circulaire, évaporation, gestion intégrée des déchets, réhabilitation des résidus miniers

1. Introduction

Mining activities produce several gigatons of mine waste yearly (Bussière and Guittonny 2021) and the observed increases in high tonnage and lower-grade deposits exploitation will further intensify the generation of mine waste (Reichl et al. 2017; Tayebi-Khorami et al. 2019). The mine waste storage areas which consist of tailings storage facilities (TSF) and waste rock stockpiles can exceed several hundreds of hectares in surface (Amos et al. 2015). The environmental impact of those large structures can cause the geochemical and the geotechnical stability issues (Rico et al. 2008; Aubertin 2013; Islam and Murakami 2021). One of the main challenges of mine waste management concerns geochemical processes, as the weathering of sulfidic tailings can lead to acid mine drainage (AMD) when exposed to the oxygen and water (Aubertin et al. 2016). The resulting leaching water generally contains high concentrations of sulfates, metals, and metalloids and is characterized by low pH (Nordstrom et al. 2015).

Various reclamation methods have been developed through cover techniques and/or the control of the water table position to prevent AMD. These methods limiting one of the components of the oxidation reactions (i.e., water, oxygen, or sulfides) to very low concentrations. Under humid and temperate climate (i.e., positive water balance), controlling oxygen fluxes is one of the most sustainable approaches (Aubertin et al. 2016). The rate of oxygen diffusion can be controlled by reducing the bulk diffusion coefficient of the tailings through the control of the degree of saturation of the medium, since oxygen diffusion is 10 000 times smaller in water than in air (Demers et al. 2009; Mbonimpa et al. 2011). This can be achieved by maintaining the saturation of the tailings through the elevated water table technique combined with a monolayer cover (EWT; Pabst 2021). The water table can be maintained through various methods, such as constructing spillways, partially impervious dams and installing an impermeable layer under the tailings prior their deposition (Pabst 2021). The monolayer cover can consist of either fine-grained or coarse-grained material.

Fine-grained covers can maintain a high degree of saturation and therefore further reduce the oxygen fluxes (oxygen barrier) through the tailings, but are strongly susceptible to evaporation (Pabst et al. 2018). Seasonal fluctuations in the degree of saturation of the underlying tailings and fine covers occur due to wetting and drying variations, potentially impacting the performance of the covers (Demers et al. 2010). In addition, the increasing frequency of dry periods resulting from climate change may further impact the performance of cover systems (Lieber et al. 2022). Controlling the water balance, and more specifically the evaporation, will become a critical factor in the design of the reclamation technique and the assessment of its long-term performance. The installation of coarse-grained layer (evaporation barrier) can increase the performance of covers (Pabst et al. 2018) and is therefore imperative. Typically, a coarse-grained dry cover, where a capillary break forms with the underlying fine materials, reduces evaporation and increases infiltration (Ouangrawa et al. 2009, 2010). Therefore, the control of the water balance can be optimized by adding a cover made of coarse material on the top on the tailings or the fine-grained layer (bilayer).

1.1. Evaporation mechanisms

Evaporation is generally divided into two stages, stage I being dominated by water flow and stage II by vapour flow (Or et al. 2013). During stage I, the evaporation rate (E_a) is nearly constant and close to potential evaporation (E_p), the media is fully saturated, and the evaporation ratio (E_r) is maintained at 1 (i.e., $E_r = E_a/E_p = 1$). Therefore, stage I is mainly controlled by the atmospheric demand. Evaporation can be maintained by a capillary rise to the surface in hydraulically connected saturated pores (Shokri and Salvucci 2011), until the hydraulic connection between the receding drying front and the soil surface begins to disconnect (Li et al. 2019). The evaporation process is governed by the capillary pressures inherent in the material, specifically the air entry value of the water retention curve and the critical capillary pressure, which corresponds to the residual volumetric water content at which the hydraulic connection is disrupted. Fine soils generally exhibit higher evaporation rates and can maintain stage I for a longer period than coarser soils, because of greater water retention capacity (Or et al. 2013).

The transition phase between stage I and II consists of a decrease in the degree of saturation of the soil and actual evaporation becomes more and more limited by the supply of water to the surface. Actual evaporation decreases and becomes lower than the potential evaporation, and the evaporation ratio is therefore less than 1. The drying front depth is determined by the pore size distribution of the porous media (Lehmann et al. 2008). In the case of heterogeneous materials, the difference in the pore size can form a drying front that propagates preferentially in the coarse pores, while the fine-pore domain remains saturated and hydraulically connected (Lehmann and Or 2009). The capillary upward liquid flow provided by the fine fractions can effectively maintain hydraulic connection between the shallow water table and the surface (Shokri and Salvucci 2011). The soil texture, permeability curves, water retention curves also contribute to the dynamics of actual evaporation (Or et al. 2013; Lehmann et al. 2018). During stage II, the drying front moves downwards, and liquid water can no longer reach the surface by capillary forces. The water contained in the pores becomes discontinuous and water transport is governed by vapour movement through gas diffusion (Saito et al. 2006), in response to a gradient of partial vapour pressure. Vapour unit flux can be expressed, for isothermal conditions (Dobchuk et al. 2004):

$$q_v = -n_a D^* \frac{\mu_v}{RT} P_s \frac{\partial RH}{\partial z} \quad (1)$$

where n_a is the air porosity (−), D^* is the diffusion coefficient of water vapour in air (m^2/s), μ_v is the molecular mass of water vapour (0.018 kg/mol), R is the universal gas constant (8.314 J/mol/K), T is the absolute temperature (K), P_s is the saturated vapour pressure (Pa), and RH is the relative humidity (−).

1.2. Waste rock as an evaporation barrier

Evaporation barriers generally consist of a layer of coarse material that can restrict upward capillary water flow and only allow upward transport of water in the vapour phase through diffusion processes (stage II), thereby sustaining a low evaporation rate (Dagenais 2005; Ouangrawa et al. 2010). Typically, evaporation barriers in cover systems are made of sand and gravel. However, the construction of these covers often requires large quantities of coarse materials, extracted from borrow pits and may have to be transported over long distances to the mine site, with a significant ecological footprint (Park et al. 2018; Aubertin et al. 2016). Recent research on integrated mine waste management has investigated opportunities to reuse non-reactive waste rocks for diverse purposes in the framework of sustainable mining practices (Demers and Pabst 2021). These applications include reusing waste rock for the construction of mine haul roads (Laverdière et al. 2023), for drainage inclusions in tailings storage facilities (Saleh-Mbemba et al. 2019), for backfilling in pits or underground mines (Li et al. 2019) and as the constitutive material in covers systems for the reclamation of mine sites such as cover with capillary barrier effects and bilayer combined with the EWT (CCBE; Larochelle et al. 2019; Pabst et al. 2017*a*; Kalonji Kabambi et al. 2017). Reusing material such as waste rock offers a significant advantage by effectively reducing the volume of waste deposited in the stockpiles and decreasing reclamation or management costs (Park et al. 2018). Therefore, waste rock could be potentially reused in such covers as an evaporation barrier.

The reuse of waste rock as an evaporation barrier raises technical challenges that must be addressed to optimize their potential valorization. Waste rock is a heterogeneous well-graded material with particle size ranging from micrometres to meters (Amos et al. 2015). Waste rock contains typically 10%–30% of particles smaller than 4.75 mm. In general, the fine fraction controls the flow regime (Amos et al. 2015), except sometimes during sporadic high precipitations events where macropores flow can dominate (Neuner et al. 2013; Fretz 2013). The fraction [0; 4.75 mm] influences the shape of the water retention curve and the air-entry value of the waste rock, and thus the capillarity properties (Amos et al. 2015). Waste rock having greater than 20% by mass of finer than 2 mm and 40% finer than 4.75 mm can exhibit *soil-like* behaviour where the dominant mass transport is through matrix flow (Smith et al. 1995; Barbour et al. 2016; Neuner et al. 2013).

An evaporation barrier made of waste rock would therefore be highly sensitive to the percentage of fine particles (Ouangrawa et al. 2010). In addition, waste rock is frequently acid generating with the fine fractions controlling the reactivity (e.g., <4.75 mm; Sylvain et al. 2024), posing a challenge to its potential for reuse. The sieving and removal of the fine fractions from the waste rock can help to mitigate their reactivity and potentially expand the reuse potential of greater quantity of waste rock (Elghali et al. 2019; Sylvain et al. 2024). Furthermore, maintaining hydraulic connections from the underlying reactive pre-oxidized tailings and the cover by the fine portions of the waste rock in case of shallow water table would compromise the water quality in the cover by allowing upward capillary flow of contaminated water. A better understanding of the effect of particle size on the performance of an evaporation barrier would therefore contribute to optimize the design of engineered cover systems. Such information would provide operators practical tools to adapt blasting patterns or select more adequately well adapted waste rock to maximize their reuse. In this research, the effects of the fine particles were addressed using an experimental approach combined with numerical modelling to optimize the particle size distribution (PSD) of an evaporation barrier. This paper presents the performance results of three covers made from different fractions of waste rock: a total fraction F0[0;37,5 mm], a medium fraction F5[5;37.5 mm], and a coarse fraction F10[10;37.5 mm], which were used to prevent evaporation from saturated tailings. Experimental results were then compared with numerical simulations.

Table 1. Physical properties of the tested materials.

Material	d_{10} (mm)	d_{30} (mm)	d_{60} (mm)	C_u (−)	G_s (−)	k_{sat} (m/s)
Ta	0.003	0.012	0.041	13	2.71	$1{\cdot}10^{-7}$
F0	0.07	3.0	12.2	174	2.92	$4{\cdot}10^{-3}$
F5	6.8	11.3	19.2	3	2.89	$1{\cdot}10^{-2}$
F10	11.8	15.6	23.4	2	2.89	$5{\cdot}10^{-2}$

2. Materials and methods

2.1. Waste rock and tailings properties

The tailings Ta were sampled directly after production and the waste rock WR were sampled in situ in the waste rock piles. The tailings (Ta) and the three waste rock fractions (WR) were extensively characterized in the laboratory (Table 1). Specific gravity (G_s) of the waste rock was measured according to ASTM C127 (2015) and the specific gravity of the tailings was measured using a helium pycnometer (Micrometrics AccuPyc 1330) and both represented typical values of hard rock mine wastes (Bussière 2007). The PSD of the tailings was obtained using laser diffraction analysis (Malvern Mastersizer). PSD of the total waste rock samples F0[0;37.5 mm] was determined according to ASTM D6913 (2021). Two fractions F5[5;37.5 mm] and F10[10;37.5 mm] were then prepared by sieving out the fine particles of the total fraction F0 (Table 1).

Tailing Ta were exhibiting typical distribution of hard rock tailings (Bussière 2007), with d_{10} of 0.003 mm and of d_{60} of 0.041 mm (where d_x is the diameter at x% of grains passing on the cumulative PSD curve). The total fraction F0, the sieved fraction F5 and F10 were coarser than the fine-grained tailings Ta (e.g., d_{60} of 12.2 mm, 19.2 mm and 23.4 mm, respectively for F0, F5, and F10 compared to 0.041 mm for the tailings Ta). However, the fraction F0 contained 37% of particles smaller than 4.75 mm and more than 20% passing the 2 mm sieve, which characterized the fraction F0 as "*soil-like*" waste rock (Barbour et al. 2016). Hydraulic properties such as the water retention curve, the air-entry pressure and the residual saturation of waste rock are primarily governed by the fraction smaller than 5 mm (Yazdani et al. 2000).

Fig. 1. (*a*) Water retention curves measured in the laboratory and predicted with modified Kovacs model (Aubertin et al. 2003), and (*b*) calculated hydraulic conductivity functions of tailings Ta and waste rock fractions F0, F5, and F10.

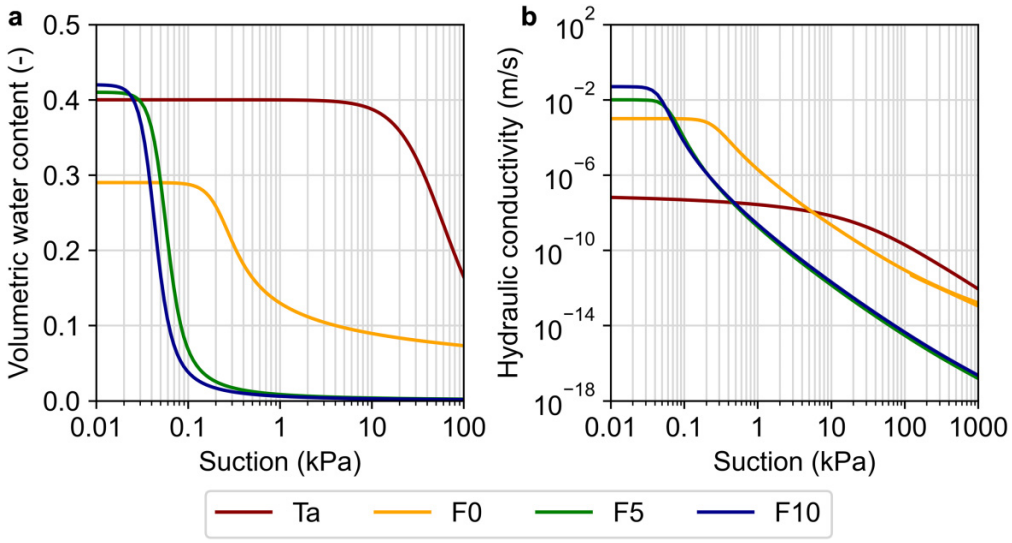

Table 2. Parameters used in the numerical model where a_{vG}, m_{vG}, and m_{vG} are van Genuchten shape parameters, θ_s the volumetric water content at saturation, θ_r the residual volumetric water content, a, m_{fx} and m_{fx} are Fredund and Xing fitting parameters and k_{sat} the hydraulic conductivity at saturation.

Tailings	van Genuchten (1980) fitting parameters					k_{sat} (m/s)
	a_{vG} (kPa)	θ_s (−)	θ_r (−)	m_{vG} (−)	n_{vG} (−)	
Ta	40.8	0.45	0	0.47	1.9	$1{\cdot}10^{-7}$
Waste rock	**Fredlund and Xing (1994) fitting parameters**					**k_{sat} (m/s)**
	a (kPa)	**θ_s (−)**	**m_{fx} (−)**	**n_{fx} (−)**		
F0	0.2	0.29	0.5	3.5		$1{\cdot}10^{-3}$
F5	0.05	0.41	1.4	5.3		$1{\cdot}10^{-2}$
F10	0.04	0.42	1.5	5.4		$5{\cdot}10^{-2}$

The hydraulic conductivity of the tailings was measured in the field using a Guelph permeameter (Chai-Onn and Pabst 2023) and was compared with the predictive method by modified Kozeny–Carman model (KCM; Mbonimpa et al. 2002). The hydraulic conductivity of waste rock fractions F0, F5, and F10 were determined using permeability tests conducted in columns and results were compared to the Taylor (1948) model. The hydraulic conductivities of all waste rock fractions were 4–5 orders of magnitude greater than the tailings (Table 1), suggesting favourable hydraulic properties for a capillary break.

The water retention curve of the tailings was measured in the laboratory by Chai-Onn and Pabst (2023) using a 15-bar pressure plate extractor (SoilMoisture Equipment Corp.) and the measured value were compared with the Modified Kovacs (MK) predictive model. The tailings water retention curve was expressed using the van Genuchten (1980) equation and the hydraulic conductivity function were calculated with the Mualem (1976) model (Fig. 1). The air-entry pressure of the tailings was approximately 20 kPa. The water retention curve of the waste rock was obtained by conducting a wetting test along with a free drainage test (Peregoedova et al. 2014) and compared to the predictive model MK (Aubertin et al. 2003) adapted by Fredlund and Xing (1994) model was used in the numerical model to represent the water retention curves and the permeability function of the waste rock to improve the convergence of the numerical model (Table 2). The air-entry pressure of the fraction F0 was 0.3 kPa and fractions F5 and F10 exhibited similar water retention characteristics and their air-entry pressure, respectively, 0.04 and 0.025 kPa.

2.2. Evaporation column experiments

Three large, instrumented columns were set up in the laboratory to perform evaporation tests (Fig. 2). Each column was 1 m high and had an internal diameter of 0.30 m (i.e., 8 times the maximum particle diameter, as recommended by Chapuis (2012). The tailings were deposited at a gravimetric water content of 17 ± 1% and compacted at a porosity of 0.45. A 40 cm thick evaporation barrier made of waste rock was placed dry on the top of the tailings, with a porosity of 0.29 for the total fraction (F0), and 0.44 for the coarse fractions (F5 and F10). Instrumentation of the columns included volumetric water content sensors (VWC; sensor types 5TM, EC-5 and Teros 12; ±0.03 m^3/m^3) and suction probes (Watermark 200SS; ±1 kPa) installed at z = 0.1, 0.30, and 0.55 m in

Fig. 2. Configuration of the evaporation column tests.

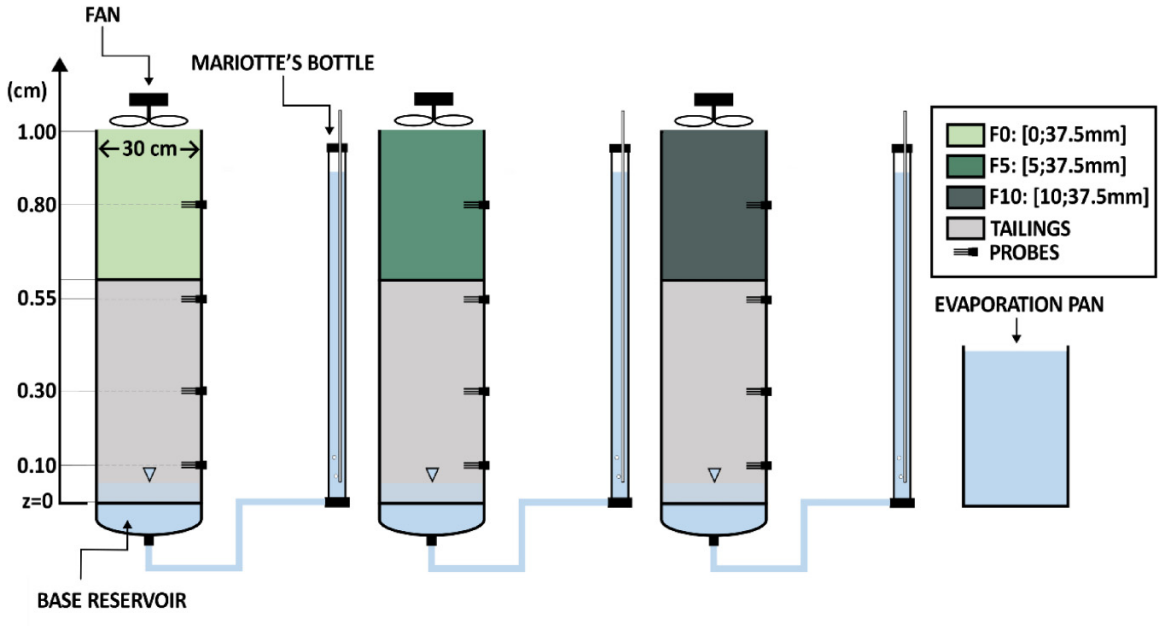

the tailings and $z = 0.8$ m in the waste rock (Fig. 2). VWC were calibrated individually prior to their installation for each type of material and type of sensors.

Three evaporation tests (T1–T3) were carried out at the laboratory to simulate drought periods: T1 was 72 days, T2 was 71 days, and T3 was 50 days long. Fans were installed at the top of the columns to maximize evaporation. All columns were connected to a Mariotte's bottle to simulate a constant water table position at $z = 0.05$ m (i.e., from the bottom of the tailings) for Test 1 and Test 3 and 0.2 m for Test 2. Mariotte's bottles had a diameter of 0.0508 m and a height of 2.0 m and were also used to estimate water loss to evaporation. Potential evaporation from an open water surface (E_p) was measured using a 0.3 m diameter evaporation pan also installed under a fan (Fig. 2). The evaporation pan was placed on a scale to measure water mass loss. Ambient relative humidity (RH) and temperature (T) were monitored every 15 minutes during the tests using a humidity and temperature sensor (Lascar EL-USD-2-LCD EasyLog USB).

The simulation of evaporation rates in the cover systems was conducted using SEEP/w model (GeoStudio 2022). Laboratory column tests were represented by a 1D model with a mesh size of 0.5 mm for the covers and 1 mm for the tailings. Convergence criteria were established with a maximum pressure head difference between two iterations of 5 mm.

Adjustments to the under-relaxation criteria were necessary due to the nonlinearity of the input material functions. The hydraulic conductivities of the cover materials were varied by several orders of magnitude over a small pressure range (i.e., the steep slope of the curve; Fig. 1*b*), so the magnitude of change of the pore-water pressure from one iteration to the next was constrained by the following equation:

$$(2) \qquad u_n^* = u_{n-1} + \alpha\,(u_n - u_{n-1})$$

where u_{n-1} is the previous iteration pore-water pressure, u_n is the tentative pore-water pressure and u_n^* is pore-water pressure. The under-relaxation parameter α was set at an initial rate of 0.55 with a minimal rate of 0.01 and a reduction factor of 0.65. The frequency of the reduction factor was set at five iterations. This ensured model stability but increased resolution time.

A Dirichlet (Type one) condition was imposed at the base of the columns to simulate the constant water table position. The land climate interaction (LCI) boundary condition was used for the transient analysis. The following user-defined LCI boundary condition was used:

$$(3) \qquad q_{AE} = q_{PET}\left[\frac{p_v^s - p_v^a}{p_{v0}^s - p_v^a}\right]$$

where q_{PET} is the measured potential evaporation, p_v^s and p_v^a are the vapour pressure of the surface and the air above the material, respectively, and p_{v0}^s is the vapour pressure at the surface of the material at saturation. The average daily humidity and temperature were calculated and implemented in the LCI boundary conditions (Fig. 3). Isothermal vapour flow was coupled to the water transfer with SEEP/w in the numerical models. The surface temperature was assumed to be equal to the air temperature during the simulations. The minimum pore-water pressure function used was calculated via the LCI boundary conditions. This function determines the minimum pore-water pressures achievable at the soil–air interface, based on the average humidity, h_a:

$$(4) \qquad u_w^{min} = \frac{\rho_w RT}{M}\ln(h_a)$$

where u_w^{min} is the minimum pore-water pressure at the soil–air interface, ρ_w is the mass density of water (g/m^3), R is the

Fig. 3. Monitored daily temperature, daily relative humidity in the laboratory during the (*a*) Test 1, (*b*) Test 2, and (*c*) Test 3.

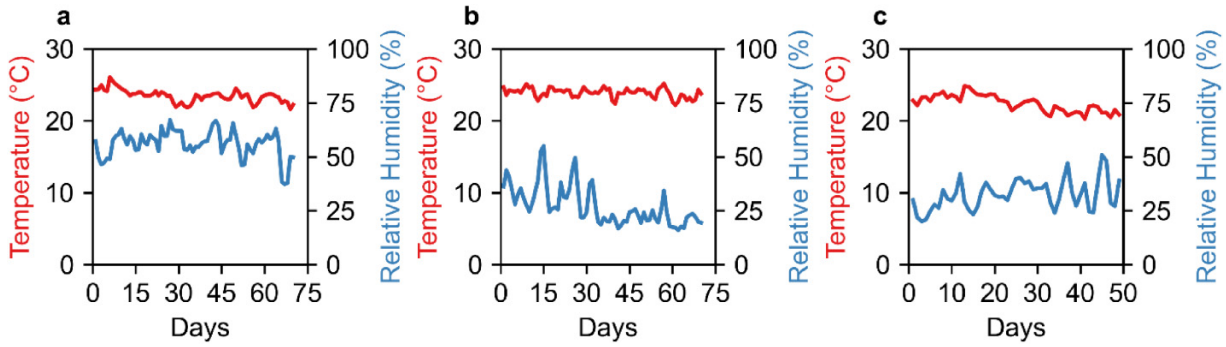

gas constant 8.314 J/K/mol, T is the temperature in Kelvin (K), and M is the molecular mass of water. For example, the air relative humidity of 0.5 at a temperature of 20 °C corresponds to a pore-water pressure of −95 045 kPa.

The simulations were calibrated based on the ability of the model to reproduce the hydrogeological behaviour of the column tests. The numerical results of the volumetric water content and suction were evaluated based on their overall agreement with laboratory measurements. The numerical cumulative evaporation results of all tests were compared to the laboratory results using the root mean square error (RMSE) and the mean absolute error (MAE). The objective was to minimize RMSE and MAE, which are indicative of higher accuracy and ensure a closer agreement between numerical simulations and laboratory results.

2.3. Parametric study and influence of fines

Following the calibration of the numerical model on laboratory test results, a parametric study was conducted to evaluate the impact of the thickness of the covers and of the water table position on the cover performance. The thickness of the covers simulated ranged from 0.4 to 2 m, (typical thickness for covers; Ouangrawa et al. 2005; Demers et al. 2008). Additional thickness of 3 and 4 m were also simulated to evaluate the possibility of increasing the reuse of waste rock. The performance results were compared in terms of water balance, more particularly the cumulative evaporation.

A second parametric study was also conducted to evaluate the impact of the fine content on the evaporation rate. The PSD function of the total sample (0; 37.5 mm) was adjusted using the Levenberg–Marquardt nonlinear algorithm (Marquardt 1963) applied on the parameters g_a, g_n, d_m, g_m, and d_r of the Fredlund (2000) equation:

$$(5)\qquad P_d = \left(\frac{1}{\ln\left(\exp(1)+\left(\frac{g_a}{d}\right)^{g_n}\right)^{g_m}}\right)\left(1-\left(\frac{\ln\left(1+\frac{d_r}{d}\right)}{\ln\left(1+\frac{d_r}{d_m}\right)}\right)^{7}\right)$$

where g_a represent a parameter related to the initial breaking point of the PSD curve, g_n represent a parameter related to the steepest slope of the curve, g_m is the parameter related to the shape of the fines portion of the curve, d_r is the parameter related to the amount of the fine portions, and d_m is the diameter of the minimum allowable particle size and d is the diameter of particle size.

A range of representative PSDs of waste rock was considered. Twenty-two synthetic PSD curves were then generated using the Fredlund (2002) equation and by adjusting the minimum particle size diameter, d_m, and maintaining all other parameters to conserve the coarser part of the original curve (5; 37.5 mm). Hydraulic conductivities were estimated by Taylor model (1948) model MK_s model was used to estimate the water retention curve (Peregoedova et al. 2014). The Fredlund and Xing (1994) model was used to describe the predicted WRCs and determine the corresponding permeability functions in the numerical simulations.

3. Results

3.1. Laboratory hydrogeological response

Laboratory column test results showed a significant impact with regard of the PSD of the waste rock on the hydrogeological response of the cover. A hydraulic connection was observed between the tailings to the cover F0 during the tests. The water table position varied from 0.05 to 0.2 m (during the tests), with corresponding suction measurements in the cover F0 (middle) ranging between 6 and 9 kPa, indicating conditions close to the hydrostatic equilibrium. Furthermore, the water content in the waste rock increased from dry (initial state) to 0.09 m^3/m^3, corresponding to a degree of saturation of 31% at the beginning of the tests (increase of the water table to initial position, before the evaporation test started). This confirmed that a hydraulic connection was formed between the fine portions of the waste rock and the tailings, suggesting an upward capillary flow of water, and corroborating the suction measurements closes to the hydrostatic equilibrium prior to testing.

For the coarse materials F5 and F10, suction measurements remained at a dry state (the maximum value of the probes is 254 kPa). This suggests the presence of an effective capillary break between these coarse covers and the tailings, preventing any water from rising by capillary action. The covers made of coarse material F5 and F10 remained dry during all tests (<0.03 m^3/m^3). The hydrogeological properties of dry covers presented steep water retention curves with low air-entry pressure of 0.03 and 0.04 kPa (Fig. 1*a*). The hydraulic

Table 3. Variations of VWC in the tailings and the covers for Tests 1, 2, and 3.

Material	Elevation	VWC (–)	F0			F5			F10		
			Test 1	Test 2	Test 3	Test 1	Test 2	Test 3	Test 1	Test 2	Test 3
WR	80 cm	Minimum	0.07	0.08	0.09	Dry	Dry	Dry	Dry	Dry	Dry
		Maximum	0.08	0.09	0.10						
Ta	55 cm	Minimum	0.40	0.39	0.39	0.44	0.44	0.43	0.44	0.44	0.45
		Maximum	0.43	0.42	0.42	0.47	0.46	0.45	0.47	0.46	0.46
Ta	30 cm	Minimum	0.37	0.38	0.38	0.42	0.43	0.44	0.46	0.46	0.47
		Maximum	0.39	0.38	0.39	0.44	0.44	0.45	0.47	0.49	0.48
Ta	10 cm	Minimum	0.38 0.41	0.39	0.39	0.39	0.37	0.38	0.40	0.40	0.40
		Maximum	0.41	0.40	0.40	0.41	0.42	0.40	0.41	0.41	0.41

Note: VWC, volumetric water content sensors.

Table 4. Daily average flow in the middle (0.8 m) of the covers.

Flow	F0			F5			F10		
	Test 1	Test 2	Test 3	Test 1	Test 2	Test 3	Test 1	Test 2	Test 3
Water flow ($m^3/s/m^2$)	$6{\cdot}10^{-9}$	$9{\cdot}10^{-9}$	$6{\cdot}10^{-9}$	$2{\cdot}10^{-16}$	$1{\cdot}10^{-16}$	$1{\cdot}10^{-16}$	$2{\cdot}10^{-16}$	$1{\cdot}10^{-16}$	1×10^{-16}
Vapour flow ($m^3/s/m^2$)	$4{\cdot}10^{-14}$	$3{\cdot}10^{-14}$	$4{\cdot}10^{-14}$	$4{\cdot}10^{-10}$	$6{\cdot}10^{-10}$	$6{\cdot}10^{-10}$	$4{\cdot}10^{-10}$	$7{\cdot}10^{-10}$	6×10^{-10}

conductivity decreased abruptly at low suction and generated a marked capillary break between the tailings and the dry covers, preventing the upward capillary flow (Fig. 1*b*). This is consistent with the constant dry VWC and the high suction (dry).

The water table position was constant during all tests, confirmed by the suction measured at the bottom of tailings was 0 kPa throughout the tests. Water content of tailings remained constant and close to saturation during all tests in the columns and at every elevation (10 cm; 30 cm; 55 cm). Small variations of ± 0.03 m^3/m^3 were observed but were deemed negligible due to the accuracy of the sensors (Table 3). The volumetric water content of the waste rock remained relatively constant throughout each test, and volumetric water content variations of ± 0.03 m^3/m^3 were also observed.

3.2. Evaporation rates

The average potential evaporation rates in tests 1, 2, and 3 were 5.1, 8.9, and 6.6 mm/day, respectively (Fig. 5). These rates corresponded to a cumulative potential evaporation of 385 mm for Test 1, 640 mm for Test 2, and 315 mm for Test 3 (Fig. 5). The higher potential evaporation rate was recorded during Test 2 because of the lowest relative humidity (Fig. 3*b*). Daily potential evaporation rate variations were recorded in the laboratory, ranging from 3.1 mm/day to a maximum of 11 mm/day.

Actual evaporation rates in columns with fractions F0, F5, and F10 were at least one order of magnitude lower than the potential evaporation (Fig. 6). For example, during Test 2, the average actual evaporation F0 was 0.7 mm/day and approximately 0.1 mm/day for columns F5 and F10, while the potential evaporation rate was 8.9 mm/day. The maximum actual evaporation recorded during Test 2 was 1.6 mm/day (at day 28), corresponding to an evaporation ratio of 0.2. The total cumulative actual evaporation was greater for F0 than for F5 and F10 (Fig. 6). For instance, the total cumulative evaporation measured in F0 for Test 2 reached 60 mm, which was significantly greater than the cumulative evaporation of 7 mm measured in the coarse covers F5 and F10. The evaporation ratio in F0 varied between 0.05 and 0.2 during Test 1, between 0.02 and 0.2 during Test 2 and between 0.03 and 0.1 during Test 3.

Evaporation rates in covers F5 and F10 were therefore reduced by a factor of approximately 90 compared to the potential evaporation. The maximum actual evaporation measured was 0.1 mm/day in F5 for Test 1. Both cover F5 and F10 remained fully dry. The overall performance of these dry covers (F5 and F10) in reducing evaporation was similar. The evaporation ratio of both columns ranged from 0 to 0.1 for Test 1 and 0 to 0.07 for Test 2 and Test 3

3.3. Numerical modeling

The numerical simulations were able to accurately replicate the measured cumulative potential evaporation. Numerical results were precise for Test 2 (exactly 640 mm) but tended to underestimate cumulative potential evaporation by around 15 mm (i.e., 5%) for Test 1 and Test 3. RMSE and MAE confirmed the good accuracy of the simulations and were for example smaller than 3 mm for the cumulative evaporation for F0 (Figs. 7*a*–7*c*). The evaporation ratios were close to the laboratory measurements. For example, in F0, evaporation ratios were between 0.08 and 0.2 in the simulations and between 0.02 and 0.2 at the laboratory.

The low cumulative evaporations measured for coarse covers F5 and F10 were generally also well simulated by the numerical model for all tests with differences between modelled and observed values usually less than 4 mm over a period of 70 days (Figs. 7*d*–7*i*). The model tended to underestimate the cumulative evaporation in the column F5 and F10 by 2–3 mm. The (limited) difference may have been caused by advective

Fig. 4. (*a*) Synthetic particle size distribution with different fine particles contents; and (*b*) corresponding water retention curves estimated using MK_s and fitted using Fredlund and Xing (1994) model.

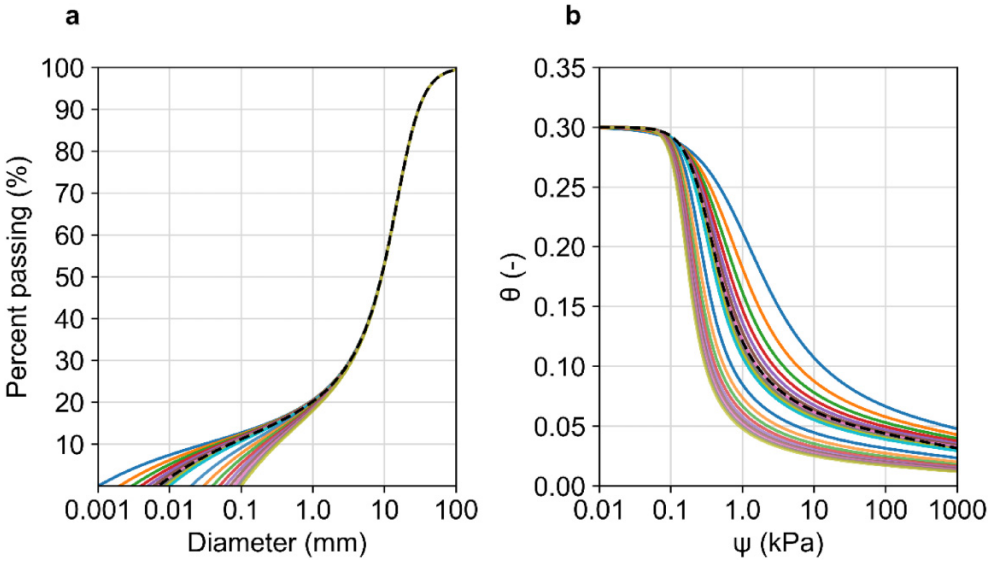

Fig. 5. Total potential evaporation for Test 1 (T1), Test 2 (T2), and Test 3 (T3).

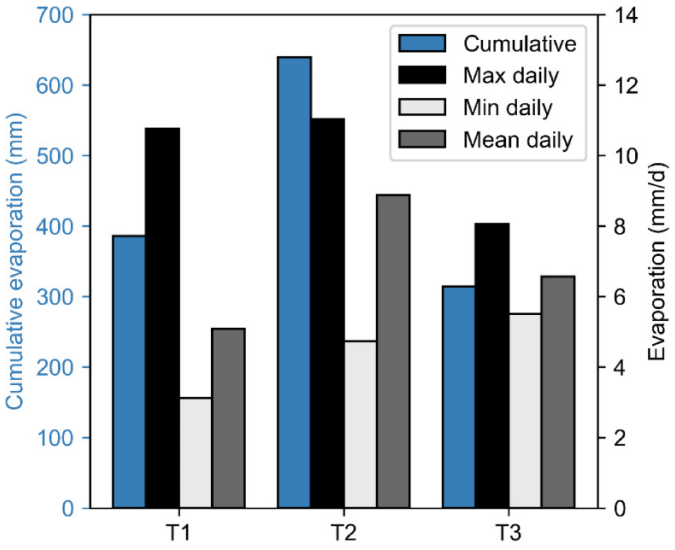

fluxes which were not included in the simulations and may have led to an underestimation of the gas movement (Vriens et al. 2018), and in this case vapour movement.

Simulations also accurately represented the variation of VWC in all the covers, with differences usually smaller than 0.03. For example, in the cover F0, the VWC remained stable at 0.09 m^3/m^3, which was similar to the VWC measured in the laboratory (0.08–0.10 m^3/m^3). VWC in the coarse covers (F5 and F10) remained close to residual VWC 0.03.

The model consistently yielded slightly higher suctions (+3 kPa at maximum, that is less than 9.5% difference) compared to the laboratory measurements in the cover F0. For example, the suction measured during Test 3 was 8 to 9 kPa ± 1 kPa, and in the numerical model, the suction remained at 11 kPa.

Simulated water flow in the cover F0 generally exceeded vapour flow by 5–6 orders of magnitude during all tests (Table 4). For example, the daily averaged flow of vapour was around $1{\cdot}10^{-14}$ $m^3/s/m^2$, i.e., much lower than water flow ($1{\cdot}10^{-9}$ $m^3/s/m^2$) for F0 cover. The highest flow of water was observed during Test 2, because of the higher potential evaporation rate. Vapour flow diffusion was the primary mechanism simulated in the dry and coarse covers (F5 and F10). For example, vapour flows were typically 6 orders of magnitude greater than water flow varying from $4{\cdot}10^{-10}$ $m^3/s/m^2$ to $7{\cdot}10^{-10}$ $m^3/s/m^2$ in both covers F5 and F10.

4. Results analysis

4.1. Impact of cover thickness and the water table position

The influence of the cover thickness combined with different water table positions is presented for F0, as the covers F5 and F10 covers exhibited less impact due to their lower evaporation rates. Test 2 was specifically selected for its combination of the highest potential evaporation and duration (72 days). The analysis of 7 cover thicknesses (e.g., 0.4, 0.6, 0.8, 1, 2, 3, and 4 m) showed that increasing the cover thickness reduced total cumulative evaporation (Fig. 8). For example, when the water table was 0.6 m below the cover, cumulative evaporation decreased from 150 mm for a 0.4 m thick cover, to 10 mm for a 2 m thick cover. However, increasing the thickness of the cover over 2 m did not significantly increase the performance of the evaporation barrier, as cumulative evaporation remained close to 10 mm for cover thicknesses of 3 and 4 m.

The suction increased in the surface cover material as the thickness of the cover increased. The drying front corre-

Fig. 6. Actual evaporation during tests 1 to 3 for columns with covers F0, F5, and F10.

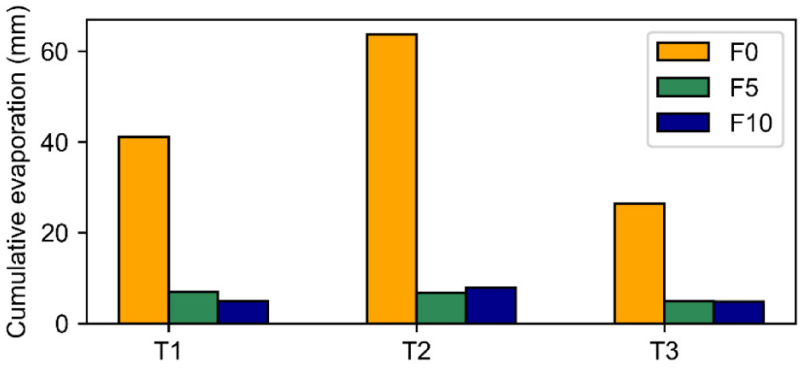

sponded to the sharp increases in suctions (pore water pressure higher than −1000 kPa). For example, at the highest water table position simulated (0.6 m), the drying front ranged from around 2–3 cm for covers 0.4, 0.6, and 0.8 m thick, to 4 cm for a 1 m cover, and ranged from 10 to 25 cm for covers 2 to 4 m thick. High suction zones within the drying front restricted water transport to vapour flow mechanisms (Dobchuk et al. 2004), significantly influencing the evaporation rate. The drying front deepens as the cover thickness increased, resulting in less cumulative evaporation. These observations corroborate similar tests in which a thin layer of desaturated material controlled the entire column evaporation fluxes due to the dominance of vapour flow instead of liquid capillary rise (Wilson 1990).

Higher water table position resulted in higher cumulative evaporation due to increased water availability. A 0.4 m thick cover was more sensitive to the position of the water table. For example, cumulative evaporation was approximately 30 mm with the lowest water table position (−0.15 m) compared to 150 mm when the water table was positioned at the interface of the cover and the tailings (0.6 m). This phenomenon is due to the transfer of suction from the water table and the hydrogeological characteristics of the covers F0 (see Fig. 1). In contrast, covers thicker than 2 m demonstrated minimum variation in cumulative evaporation, suggesting that the water position exerts a negligible influence at this magnitude of thickness for the selected material (F0). As mentioned above, in these covers, the drying front was controlling the evaporation rate. Consequently, using the total fraction of waste rock as a monolayer cover could imply enhancing the cover thickness to at least 2 m, depending on the tailings water retention properties.

4.2. Impact of the fines on evaporation

The use of numerical models to select an acceptable range of cover materials in terms of PSD could be a promising tool as a first approximation for the cover design. Specifically, the impact of the fine portions of the curves of the PSD was analyzed by generating synthetic PSD including the original PSD (i.e., PSD of the F0; Fig. 4). Therefore, a range of 20 predicted water retention curves combined predicted hydraulic conductivity was generated to evaluate the cumulative evaporation in SEEP/w (see section 2.3 for more details). Cover of 0.4 m thickness and Test 2 was chosen for the comparison, and the predicted values with the original PSD was compared with the laboratory results. Test 2 was selected for the combination of a shallow water table (0.2 m), elevated potential evaporation, and a duration of 72 days, while the cover 0.4 m was selected for its sensitivity to the shallow water table and the maximum actual evaporation.

First, the predicted saturated hydraulic conductivity calculated with the Taylor model, which is using the d_{50}, did not vary with the synthetic PSD curves (0.0012 m/s) as the upper segment of the curves was intact (black dashed curve; Fig. 4). A simulation was conducted to predict the evaporation from the original PSD. The estimated cumulative evaporation from the simulation with the original PSD was around 50 mm, which corresponded well to the cumulative evaporation of 60 mm measured in the laboratory.

Simulation results of the PSD curves with higher fines content than the original material (above the dashed black curve; Fig. 4) presented cumulative evaporation ranging from 50 to 340 mm. Evaporation increased with increasing fine content, indicating that there was more water in the cover available for evaporation. No drying front developed in the model with the material containing more fines (model with parameters; PAR1 to PAR20), as suction remained close to hydrostatic equilibrium. Evaporation was therefore only controlled by upward water flow and remained relatively high (e.g., cumulative evaporation of 340 mm). The simulated cumulative evaporation of the coarser part of the PSD (Fig. 9) was between 8 and 22 mm and tended to decrease with increasing particle size. The decrease in evaporation was attributed to the development of elevated suctions at the surfaces of the cover which resulted in the propagation of a drying front downwards. The drying front was between 4 and 17 cm deep, corresponding to a maximum cumulative evaporation of 8 mm.

Overall, simulations predicted variations in the cumulative evaporation due to the variation of the fines: the more the fines, the greater was cumulative evaporation. For the PSD range selected, cumulative evaporation was ranging from 8 to 340 mm, which could have a significant impact in the performance of the cover as an evaporation barrier.

Fig. 7. Measured (points) and simulated (line) cumulative actual evaporation in column F0 (yellow), F5 (green), and F10 (blue) for (*a*) (*d*) (*g*) Test 1, (*b*) (*e*) (*h*) Test 2, and (*c*) (*f*) (*i*) Test 3. RMSE, root mean square error; MAE, mean absolute error.

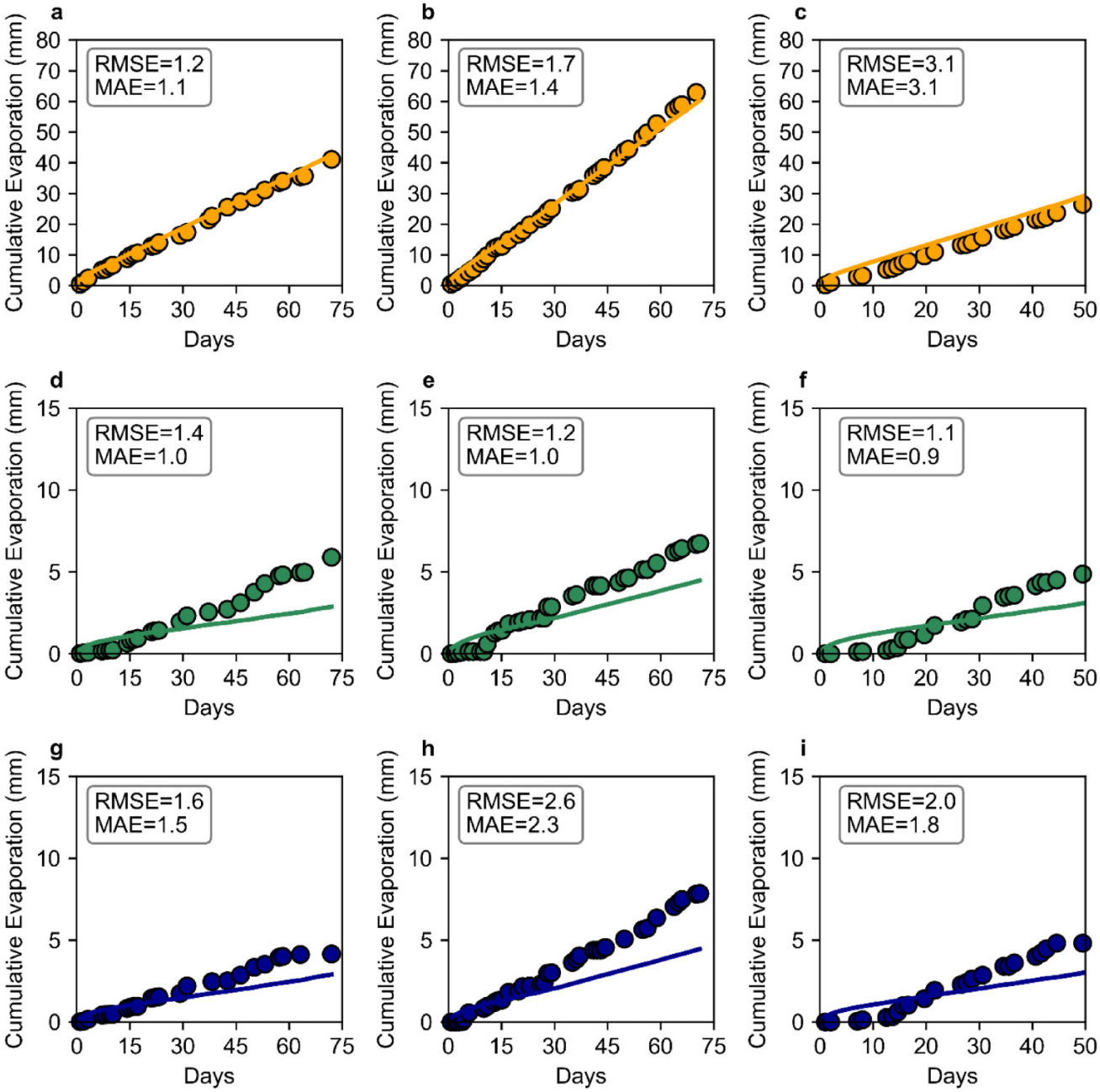

4.3. Effect of the capillary break on the evaporation barrier

The aim of this study was to compare the performance of the covers in reducing evaporation based on the proportion of fine particles in waste rock. The comprehensive analysis of VWC and suction measurements from the laboratory, along with the numerical model results conducted in F0 revealed that the proportions of fines enhanced the evaporation rates of one order of magnitude compared to the dry and coarser particle size covers in columns F5 and F10 (e.g., 1 mm/day to 0.1 mm/day). Evaporation is generally sustained for a longer period in fine soils compared to coarser and dryer soils (Or et al. 2013).

Numerical simulations performed in this study also showed that the variation of the fine part of the PSD of the waste rock (0; 5 mm) had a significant impact on evaporation. The finer PSD modelled maintained a hydraulic connection with the tailings, sustaining an upward water flow and thus increasing evaporation compared to the original PSD analyzed (F0). Cover F0 was sensitive to the water table position and the finer PSD modelled, because of their hydraulic connection with the tailings. One approach to mitigate evaporation in the cover F0 was to increase the cover thickness in the numerical simulation, as higher suction developed near the surface of the cover, which typically reduces the hydraulic conductivity in the cover (Dagenais et al. 2006). Therefore,

Fig. 8. Cumulative evaporation and the influence of the cover thickness (m), where WT is the water table position (m).

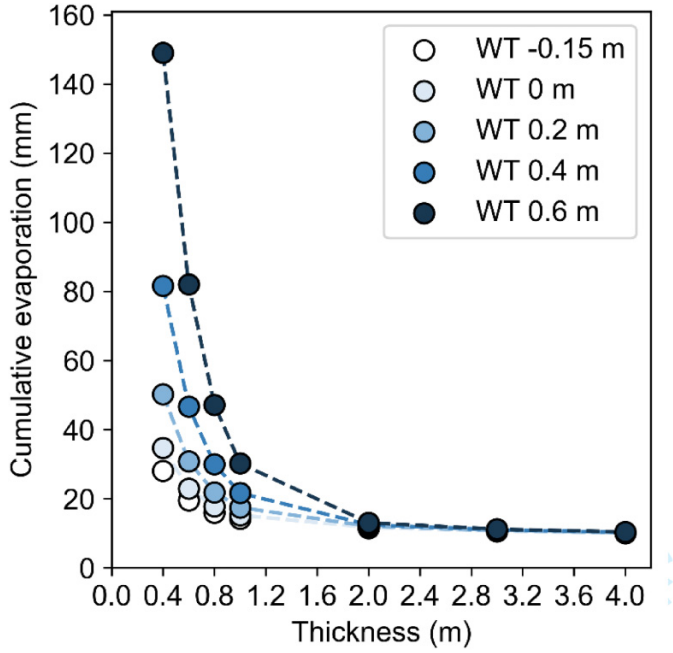

this decreases in surface saturation limited water transport via vapour diffusion, effectively minimizing evaporation. The increased in thickness contributed to minimize evaporation as suggested by Dagenais (2005) and observed for a till cover by Pabst et al. (2017*b*). A drying front could also have developed near the surface of the cover, forming a thin layer of dry soil acting as the primary evaporation control mechanism (Wilson 1990).

The coarser synthetic PSD materials typically showed low evaporation rates. The hydrogeological properties of the coarse covers F5 and F10 were characterized by low air entry value and a steep permeability function (Fig. 2*b*). These properties effectively maintained a capillary break with the tailings, preventing the upward capillary flow and thus evaporation. Evaporation in dry material was divided into three steps: (1) vaporization occurred at the surface of the tailings, (2) water diffused through the pore of the dry cover, and (3) water vapour travels to the surface to the atmosphere (Shokri and Salvucci 2011; Shokri and Or 2011). Evaporation in the coarse materials was therefore controlled by diffusion which was limiting evaporation at low rates (Dobchuk et al. 2004). The simulations indicated that vapour flow was at least three orders of magnitude greater compared with limited water flow in the middle of those dry covers. However, numerical simulations tended to slightly underestimate evaporation under vapour flow mechanisms. Sieving the fine particles helped to enhance the performance of the covers as an evaporation barrier by maintaining the evaporation ratio lower than 0.1 in all tests. Therefore, sieving part of the fines or controlling the fine content during blasting (Gao et al. 2023) could enhance the performance of the waste rock as an evaporation barrier by generating a stronger capillary break.

5. Discussion

Numerical models are important predictive and approximation tools for the first step of designing covers systems. However, simplifications of conditions and mechanisms were done to perform the calibration in this study. First, discrepancies in environmental conditions such as temperature, humidity between the laboratory setting and the model simulations may have influenced evaporation rates differently. Specifically, fluctuations in barometric pressure could have directly influenced the water table position generated by the Mariotte's bottle, thus modifying the water availability for evaporation, which was not considered in the simulations. Additionally, variations in the boundary conditions or assumptions made in the simplified numerical model compared to the physical set up in the laboratory could have contributed to the observed differences. These variations highlight the importance of careful calibration and validation of numerical models against experimental data to ensure accuracy and reliability in predictive simulations. These discrepancies also underscore the challenges in scaling from the laboratory to field applications, as larger-scale systems introduce additional environmental complexities.

The heterogeneity was modelled via equivalent homogeneous model, and the impact between the coarse pores and the fine pores could not be addressed numerically. Evaporation in heterogenous soil can be controlled by capillary flow rising only in the fine portions to the surface as observed by Lehmann and Or (2009). The presence of evaporative salt in the cover F0, particularly in regions containing fines at the surface of the laboratory column, further supports the hypothesis of capillary rise in the fine pores as salt precipitation typically occurs where water vaporizes (Yanful et al. 2003). Numerical simulations carried out with SEEP/w suggested that the primary mechanism of transport of water was by liquid capillary upward flow in the middle of the cover F0 and that near the surface in the drying front (e.g., 2 cm), diffusion of vapour was controlling the rate of evaporation.

No evaporative salt was observed at the surface of the cover F5 and F10, which indicated that the transport mechanism was mainly vapour diffusion. However, other mechanisms such as vapour condensation in the pores (Sakai et al. 2009) and sorption phenomena were not analyzed (Dobchuk et al. 2004). Thermal vapour flows were also neglected. This would impact the dynamics of the vapour fluxes and VWC of the waste rocks. Advective fluxes were not simulated in this research due to the lateral boundary from the column tests (impervious) and in the numerical model. Advection could increase evaporation rates by enhancing the transfer of water vapour form the interface of the tailings and the cover into the atmosphere, due to air displacement (Amos et al. 2009; Chi et al. 2013). This mechanism is important in coarser materials, due to the larger pore space, where the pneumatic conductivity can be high (Amos et al. 2015).

Uncertainties in the input parameters such as water retention curve, used in the numerical model, may also limit the prediction. The water retention curve of the waste rock should be better characterized, especially regarding the capacity of water retention of the fine portion of the waste rock

Fig. 9. Cumulative evaporation results from the simulations with the synthetic particle size distribution (PSD) PAR1 to PAR20 including the original PSD simulated (PSD OR) using predicting a model for the water retention curves and permeability functions. The left part represents all the curves with finer particles than the original PSD (F0). The right part represents the coarser synthetic PSD.

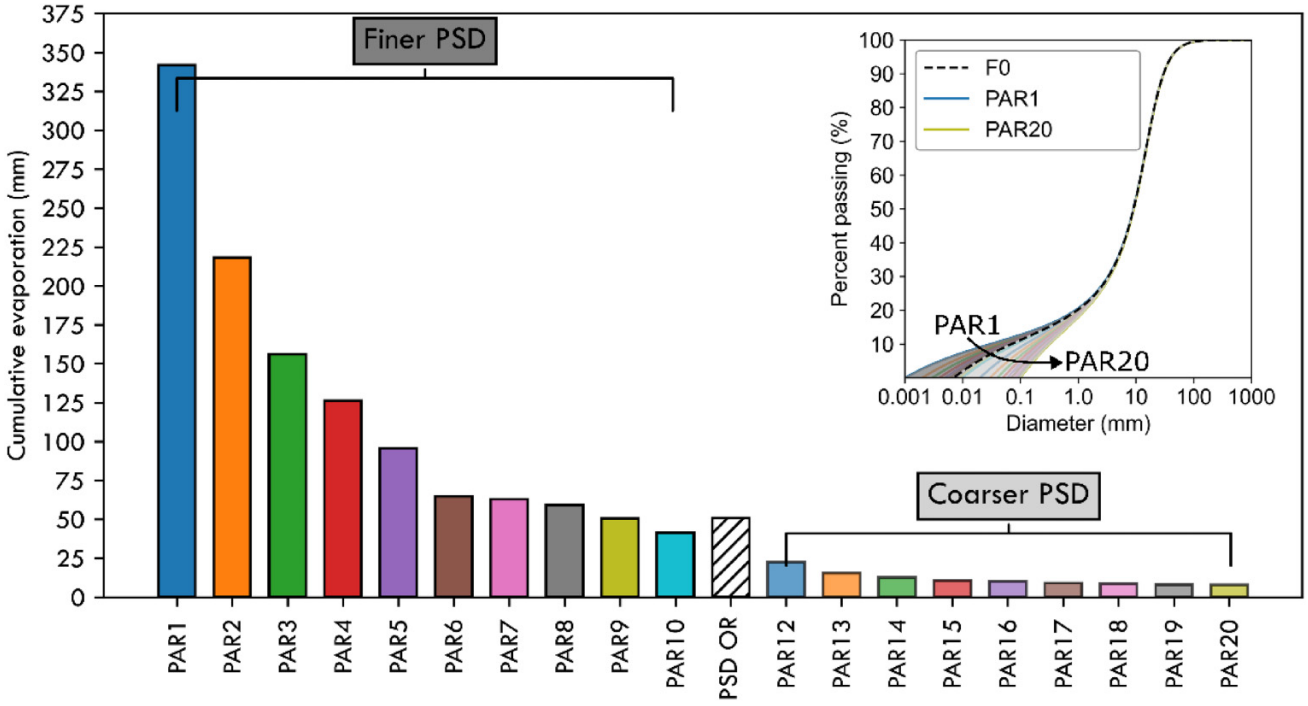

as it may play a dynamic role in evaporation processes. Predictive models and experiments pose challenges when attempting to measure the VWC using probes, especially when VWC is at residual value. Specifically, studies on predictive water retention curve and permeability function models for waste rock would help to provide valuable insights into the mechanisms driving variability in evaporation rates across cover composed of waste rock.

The monolayer cover combined with the elevated water table technique can be used for pre-oxidized tailings but typically involved a water table positioned to the surface of the tailings (Pabst et al. 2014). Capillary rise from reactive tailings to the cover could have the potential to decrease the poor water quality within the pore of covers, posing a risk to the overall effectiveness of the reclamation performance. Fine particles containing the waste rock could induce capillary flow of contaminated water, which indicated that sieving the fine portions could also be beneficial in terms of geochemistry. Furthermore, fine particles of waste rock are typically more reactive than their coarser portions (Erguler and Erguler 2015). As there is sometimes a limited quantity of non-reactive waste rock, reactive waste rock could be reused by controlling the PSD (Elghali et al. 2019). Sieving the fine particles has been shown to increase the potential of waste rock for reuse in terms of geochemistry (Sylvain et al. 2024) but further studies are needed to confirm this potential. Therefore, sieving the fine particles would not only increase the performance as an evaporation barrier as demonstrated in this study, but also increase the potential of reusing waste rock.

Highly reactive and/or pre-oxidized tailings may be sensitive to oxygen fluxes, even if the water table is sufficiently elevated (Pabst et al. 2018). A cover composed of coarser waste rock could increase oxygen fluxes towards the reactive tailings, as advection of oxygen is often observed in waste rock (Vriens et al. 2018, 2019). A protective layer of desulfurized tailings or non-reactive material could be added on the top of the reactive tailings (under the coarse-grained protective layer) to ensure that oxygen fluxes are reduced which would typically decrease the generation of contaminants (Demers et al. 2008).

6. Conclusion

The objective of this study was to assess the performance of evaporation barriers made of waste rock and more specifically the effect of the fine particle content. Three column tests were conducted in the laboratory to simulate a reclamation method involving a monolayer cover of waste rock coupled with an elevated water table. Three laboratory evaporation tests (T1 to T3) were performed. The three monolayer covers made of waste rock were tested: F0 [0;37.5 mm], F5 [5;37.5 mm], and F10 [10;37.5 mm]. The potential evaporation of free water was measured with an open water column. Generally, actual evaporation rates were at least one order of magnitude lower than the potential evaporation of free water, showing a strong reduction of evaporation because of waste rock covers. Their PSD, the water table position and the cover thickness, however, had a significant impact on the evapo-

ration barrier performance. The main findings of this study, undertaken in conditions of a shallow water table, were as follows:

- The suction in the cover with the fine (F0) was close to the hydrostatic equilibrium, which indicated a hydraulic connection between the tailings and the cover. Evaporative salts were observed at the surface of the cover F0. Therefore, there was greater water availability for evaporation in the cover F0 containing fines. Cumulative evaporation was generally 10 times higher in the F0 than in the dry covers F5 and F10.
- The coarse covers [5;37.5 mm] and [10;37.5 mm] remained dry during all the tests, suggesting a strong capillary break. No major difference in the hydrogeological behaviour was observed between those two dry covers. In these covers, vapour transport was the main mechanism, which resulted in low evaporation.
- The numerical model was performed to replicate the evaporative behaviour of those covers. Good agreement was observed between the calibrated numerical model and the laboratory measurements. Evaporation was greater in cover F0 than in the dry covers, as observed in the laboratory. The separation of water and vapour fluxes allowed for a more detailed analysis of the underlying mechanisms within the numerical model. Evaporation in dry covers was only controlled by vapour flow whereas evaporation in covers with fines by capillary rise and vapour flow.
- The numerical model revealed that the fine portions of the PSD curves of the waste rock had a significant impact on evaporation rates, as demonstrated with the parametric analysis. The finer particle was in the cover constitutive material, the more evaporation was measured. Increasing the thickness of the covers to 2 m contributed to reduce the impact of the fines on evaporation.

The fine fraction of waste rock was therefore shown to have a significant impact on the cover performance and should be considered when estimating evaporation rates and designing cover. The results of this study indicate that there is a significant opportunity to enhance the efficiency of waste rock selection and reuse processes, by selecting specific fractions of the waste rock.

Acknowledgements

We would like to thank RIME industrial partners for the sampling materials and their contributions. Additional assistance was extended by the technicians at Polytechnique Montréal and URSTM for the sampling and laboratory work.

Article information

History dates

Received: 11 September 2024
Accepted: 10 April 2025
Version of record online: 17 June 2025

Copyright

Data availability

Data generated or analyzed during this study are available from the corresponding author upon reasonable request.

Author information

Author ORCIDs

Karine Sylvain https://orcid.org/0009-0007-6630-8699
Isabelle Demers https://orcid.org/0000-0003-1406-0840

Author notes

Thomas Pabst served as Editorial Board Member at the time of manuscript review and acceptance; peer review and editorial decisions regarding this manuscript were handled by another editorial board member.

Author contributions

Conceptualization: KS, ID, TP
Data curation: KS
Formal analysis: KS
Funding acquisition: ID, TP
Investigation: KS
Methodology: KS
Project administration: ID, TP
Resources: ID, TP
Supervision: ID, TP
Validation: ID, TP
Visualization: KS
Writing – original draft: KS
Writing – review & editing: ID, TP, KS

Competing interests

The authors declare there are no competing interests.

Funding information

Financial support was provided by the Natural Sciences and Engineering Research Council of Canada (NSERC)—Alliance Grant with the participation of the Ministère des Ressources naturelles et des Forêts (MRNF), Iamgold Corporation and Agnico Eagle Mines Ltd.

References

Amos, R.T., Blowes, D.W., Bailey, B.L., Sego, D.C., Smith, L., and Ritchie, A.I.M. 2015. Waste-rock hydrogeology and geochemistry. Applied Geochemistry, **57**: 140–156. doi:10.1016/j.apgeochem.2014.06.020.

Amos, R.T., Blowes, D.W., Smith, L., and Sego, D.C. 2009. Measurement of wind-induced pressure gradients in a waste rock pile. Vadose Zone Journal, **8**(4): 953–962. doi:10.2136/vzj2009.0002.

Aubertin, M. 2013. Waste rock disposal to improve the geotechnical and geochemical stability of piles. Proc., 23rd World Mining Congress.

Aubertin, M., Bussière, B., Pabst, T., James, M., and Mbonimpa, M. 2016. Review of the reclamation techniques for acid-generating mine wastes upon closure of disposal sites. *In* Geo-Chicago 2016. pp. 343–358. doi:10.1061/9780784480137.034.

Aubertin, M., Mbonimpa, M., Bussière, B., and Chapuis, R. 2003. A model to predict the water retention curve from basic geotechnical properties. Canadian Geotechnical Journal, **40**(6): 1104–1122. doi:10.1139/t03-054.

Barbour, S.L., Hendry, M.J., and Carey, S.K. 2016. High-resolution profiling of the stable isotopes of water in unsaturated coal waste rock. Journal of Hydrology, **534**: 616–629. doi:10.1016/j.jhydrol.2016.01.053.

Bussiere, B. 2007. Colloquium 2004: hydrogeotechnical properties of hard rock tailings from metal mines and emerging geoenvironmental disposal approaches. Canadian Geotechnical Journal, **44**(9): 1019–1052. doi:10.1139/T07-040.

Bussière, B., and Guittonny, M. 2021. Hard rock mine reclamation: from prediction to management of acid mine drainage. CRC press. doi:10.1201/9781315166698.

Chai-onn, M., and Pabst, T. 2023. Experimental and numerical study of the hydrogeological behaviour of filtered tailings exposed to climatic conditions. Proceedings of the 76th Canadian Geotechnical Conference, GeoSaskatoon 2023.

Chapuis, R.P. 2012. Predicting the saturated hydraulic conductivity of soils: a review. Bulletin of Engineering Geology and the Environment **71**: 401–434. doi:10.1007/s10064-012-0418-7.

Chi, X., Amos, R.T., Stastna, M., Blowes, D.W., Sego, D.C., and Smith, L. 2013. The Diavik Waste Rock Project: implications of wind-induced gas transport. Applied Geochemistry, **36**: 246–255. doi:10.1016/j.apgeochem.2012.10.015.

Dagenais, A.-M. 2005. Techniques de contrôle du drainage minier acide basées sur les effets capillaires, École polytechnique.

Dagenais, A.-M., Aubertin, M., and Bussière, B. 2006. Parametric study on the water content profiles and oxidation rates in nearly saturated tailings above the water table. Proceedings of the 7th International Conference on Acid Rock Drainage (ICARD), **2630**: 405420.

Demers, I., and Pabst, T. 2021. Chapter 13: Alternative and InnovativeIntegrated Mine WasteManagement Approaches. Hard Rock Mine Reclamation. From Prediction to Management of Acid Mine Drainage.CRC press. pp. 321–349.

Demers, I., Bussière, B., Benzaazoua, M., Mbonimpa, M., and Blier, A. 2008. Column test investigation on the performance of monolayer covers made of desulphurized tailings to prevent acid mine drainage. Minerals Engineering, **21**(4): 317–329. doi:10.1016/j.mineng.2007.11.006.

Demers, I., Bussière, B., Benzaazoua, M., Mbonimpa, M., and Blier, A. 2010. Preliminary optimization of a single-layer cover made of desulfurized tailings: application to the Doyon Mine tailings impoundment. Society for Mining, Metallurgy, and Exploration Annual Transactions, **326**: 21–33.

Demers, I., Bussiere, B., Mbonimpa, M., and Benzaazoua, M. 2009. Oxygen diffusion and consumption in low-sulphide tailings covers. Canadian Geotechnical Journal, **46**(4): 454–469. doi:10.1139/T08-132.

Dobchuk, B.S., Barbour, S.L., and Zhou, J. 2004. Prediction of water vapour movement through waste rock. Journal of Geotechnical and Geoenvironmental Engineering, **130**(3): 293–302. doi:10.1061/(ASCE)1090-0241(2004)130:3(293).

Elghali, A., Benzaazoua, M., Bussière, B., and Bouzahzah, H. 2019. Determination of the available acid-generating potential of waste rock, part II: waste management involvement. Applied Geochemistry, **100**: 316–325. doi:10.1016/j.apgeochem.2018.12.010.

Erguler, Z.A., and Erguler, G.K. 2015. The effect of particle size on acid mine drainage generation: kinetic column tests. Minerals Engineering, **76**: 154–167. doi:10.1016/j.mineng.2014.10.002.

Fredlund, M.D Fredlund, D.G. and Wilson, G.W. 2000. An equation to represent grain-size distribution. Canadian Geotechnical Journal **37**: 4 817–827. doi:10.1139/t00-015.

Fredlund, D., Xing, A., and Huang, S. 1994. Predicting the permeability function for unsaturated soils using the soil-water characteristic curve. Canadian Geotechnical Journal, **31**(4): 533–546. doi:10.1139/t94-062.

Fretz, N.M. 2013. Multi-year hydrologic response of experimental waste-rock piles in a cold climate: active-zone development, net infiltration, and fluid flow, University of British Columbia].

Gao, P., Pan, C., Zong, Q., and Dong, C. 2023. Rock fragmentation size distribution control in blasting: a case study of blasting mining in Changjiu Shenshan limestone mine. Frontiers in Materials, **10**: 1330354. doi:10.3389/fmats.2023.1330354.

Genuchten, Van 1980. A closed-form equation for predicting the hydraulic conductivity of unsaturated soils. Soil science society of America journal, **44**(5): 892–898.

Geostudio 2022. Heat and Mass Transfer with GeoStudio.

Islam, K., and Murakami, S. 2021. Global-scale impact analysis of mine tailings dam failures: 1915–2020. Global Environmental Change, **70**: 102361. doi:10.1016/j.gloenvcha.2021.102361.

Kalonji Kabambi, A., Bussière, B., and Demers, I. 2017. Hydrogeological behaviour of covers with capillary barrier effects made of mining materials. Geotechnical and Geological Engineering, **35**(3): 1199–1220. journal article. doi:10.1007/s10706-017-0174-3.

Larochelle, C.G., Bussière, B., and Pabst, T. 2019. Acid-generating waste rocks as capillary break layers in covers with capillary barrier effects for mine site reclamation. Water, Air, & Soil Pollution, **230**(3): 1–16. doi:10.1007/s11270-019-4114-0.

Laverdière, A., Hao, S., Pabst, T., and Courcelles, B. 2023. Effect of gradation, compaction and water content on crushed waste rocks strength. Road Materials and Pavement Design, **24**(3): 761–775. doi:10.1080/14680629.2022.2044373.

Lehmann, P., and Or, D. 2009. Evaporation and capillary coupling across vertical textural contrasts in porous media. Physical Review E, **80**(4): 046318. doi:10.1103/PhysRevE.80.046318.

Lehmann, P., Assouline, S., and Or, D. 2008. Characteristic lengths affecting evaporative drying of porous media. Physical Review E, **77**(5): 056309. doi:10.1103/PhysRevE.77.056309.

Lehmann, P., Merlin, O., Gentine, P., and Or, D. 2018. Soil texture effects on surface resistance to bare-soil evaporation. Geophysical Research Letters, **45**(19): 10,398–310,405. doi:10.1029/2018gl078803.

Li, M., Zhang, J., Song, W., and Germain, D.M. 2019. Recycling of crushed waste rock as backfilling material in coal mine: effects of particle size on compaction behaviours. Physical Review E, **80**: 8789–8797. doi:10.1103/PhysRevE.80.046318.

Lieber, E., Demers, I., Pabst, T., and Bresson, É. 2022. Simulating the effect of climate change on performance of a monolayer cover combined with an elevated water table placed on acid-generating mine tailings. Canadian Geotechnical Journal, **59**(4): 558–568. doi:10.1139/cgj-2020-0622.

Marquardt, D.W. 1963. An algorithm for least-squares estimation of nonlinear parameters. Journal of the society for Industrial and Applied Mathematics **11**: 431–441.

Mbonimpa, M., Aubertin, M., and Bussière, B. 2011. Oxygen consumption test to evaluate the diffusive flux into reactive tailings: interpretation and numerical assessment. Canadian Geotechnical Journal, **48**(6): 878–890. doi:10.1139/t11-015.

Mbonimpa, M., Aubertin, M., Chapuis, R.P., and Bussière, B. 2002 Practical pedotransfer functions for estimating the saturated hydraulic conductivity Geotechnical & Geological Engineering **20**(3): 235–259. doi:10.1023/A:1016046214724.

Mualem, Y. 1976. A new model for predicting the hydraulic conductivity of unsaturated porous media. Water Resources Research **12**(3): 513–522. doi:10.1029/WR012i003p00513.

Neuner, M., Smith, L., Blowes, D.W., Sego, D.C., Smith, L.J., Fretz, N., and Gupton, M. 2013. The Diavik waste rock project: water flow through mine waste rock in a permafrost terrain. Applied Geochemistry, **36**: 222–233. doi:10.1016/j.apgeochem.2012.03.011.

Nordstrom, D.K., Blowes, D.W., and Ptacek, C.J. 2015. Hydrogeochemistry and microbiology of mine drainage: an update. Applied Geochemistry, **57**: 3–16. doi:10.1016/j.apgeochem.2015.02.008.

Or, D., Lehmann, P., Shahraeeni, E., and Shokri, N. 2013. Advances in soil evaporation physics—a review. Vadose Zone Journal, 1–16, **12**(4):. doi:10.2136/vzj2012.0163.

Ouangrawa, M., Aubertin, M., Molson, J., Zagury, G., and Bussière, B. 2005. An evaluation of the elevated water table concept using laboratory columns with sulphidic tailings. Proceedings of Geosask2005, 58th Canadian Geotechnical conference and 6th Joint IAHCNC, Saskatoon.

Ouangrawa, M., Aubertin, M., Molson, J.W., Bussière, B., and Zagury, G.J. 2010. Preventing acid mine drainage with an elevated water table: long-term column experiments and parameter analysis. Water, Air, & Soil Pollution, **213**(1-4): 437–458. doi:10.1007/s11270-010-0397-x.

Ouangrawa, M., Molson, J., Aubertin, M., Bussière, B., and Zagury, G. 2009. Reactive transport modelling of mine tailings columns with capillarity-induced high water saturation for preventing sulfide oxidation. Applied Geochemistry, **24**(7): 1312–1323. doi:10.1016/j.apgeochem.2009.04.005.

Pabst, T. 2021. Chapter 8: Elevated water table with monolayer covers. Hard Rock Mine Reclamation. From Prediction to Management of Acid Mine Drainage. CRC press(pp.187–201).

Pabst, T., Aubertin, M., Bussière, B., and Molson, J. 2014. Column tests to characterise the hydrogeochemical response of pre-oxidised acid-generating tailings with a monolayer cover. Water, Air, & Soil Pollution, **225**: 1–21. doi:10.1007/s11270-013-1841-5.

Pabst, T., Aubertin, M., Bussière, B., and Molson, J. 2017a. Experimental and numerical evaluation of single-layer covers placed on acid-generating tailings. Geotechnical and Geological Engineering, **35**(4): 1421–1438. doi:10.1007/s10706-017-0185-0.

Pabst, T., Bussière, B., Aubertin, M., and Molson, J. 2018. Comparative performance of cover systems to prevent acid mine drainage from pre-oxidized tailings: A numerical hydro-geochemical assessment. Journal of Contaminant Hydrology, **214**: 39–53. doi:10.1016/j.jconhyd.2018.05.006.

Pabst, T., Molson, J., Aubertin, M., and Bussière, B. 2017b. Reactive transport modelling of the hydro-geochemical behaviour of partially oxidized acid-generating mine tailings with a monolayer cover. Applied Geochemistry, **78**: 219–233. doi:10.1016/j.apgeochem.2017.01.003.

Park, I., Tabelin, C.B., Jeon, S., Li, X., Seno, K., Ito, M., and Hiroyoshi, N. 2018. A review of recent strategies for acid mine drainage prevention and mine tailings recycling. Chemosphere, **219**: 588–606. doi:10.1016/j.chemosphere.2018.11.053.

Peregoedova, A., Aubertin, M., and Bussière, B. 2014. Evaluation of the water retention curve of mine waste rock using laboratory tests and predictive models. Proceedings of the 67th Canadian Geotechnical Conference, Regina, Saskatchewan.

Reichl, C., Schatz, M., and Zsak, G. 2017. World-mining-data Welt-Bergbau-Daten. Federal Ministry of Science, Research and Economy, Vienna.

Rico, M., Benito, G., Salgueiro, A., Díez-Herrero, A., and Pereira, H. 2008. Reported tailings dam failures: a review of the European incidents in the worldwide context. Journal of Hazardous Materials, **152**(2): 846–852. doi:10.1016/j.jhazmat.2007.07.050.

Saito, H., Šimůnek, J., and Mohanty, B.P. 2006. Numerical analysis of coupled water, vapor, and heat transport in the Vadose Zone. Vadose Zone Journal, **5**(2): 784–800. doi:10.2136/vzj2006.0007.

Sakai, M., Toride, N., and Šimůnek, J. 2009. Water and vapour movement with condensation and evaporation in a sandy column. Soil Science Society of America Journal, **73**(3): 707–717. doi:10.2136/sssaj2008.0094.

Saleh-Mbemba, F., Aubertin, M., and Boudrias, G. 2019. Drainage and consolidation of mine tailings near waste rock inclusions. *In* Sustainable and safe dams around the world/Un monde de barrages durables et sécuritaires. CRC Press. pp. 3296–3305. doi:10.1201/9780429319778.

Shokri, N., and Or, D. 2011. What determines drying rates at the onset of diffusion controlled stage-2 evaporation from porous media? Water Resources Research, **47**(9). doi:10.1029/2010WR010284.

Shokri, N., and Salvucci, G.D. 2011. Evaporation from porous media in the presence of a water table. Vadose Zone Journal, **10**(4): 1309–1318. doi:10.2136/vzj2011.0027.

Smith, L.A., López, D.L.,Beckie, R.,Morin, K.,Dawson, R., and Price, W. 1995. Hydrogeology of waste rock dumps. British Columbia Ministry of Energy, Mines and Petroleum Resources and CANMET.

Sylvain, K., Pabst, T., and Demers, I. 2024. Improving the reuse potential of reactive waste rock using sieving: a laboratory geochemical study. Environmental Science and Pollution Research, **31**: 55490–55506. doi:10.1007/s11356-024-34679-8.

Tayebi-Khorami, M., Edraki, M., Corder, G., and Golev, A. 2019. Re-thinking mining waste through an integrative approach led by circular economy aspirations. Minerals, **9**(5): 286. doi:10.3390/min9050286.

Taylor, D.W. 1948. Fundamentals of soil mechanics. Vol. **66**. LWW.

Vriens, B., Arnault, M.S., Laurenzi, L., Smith, L., Mayer, K.U., and Beckie, R.D. 2018. Localized sulfide oxidation limited by oxygen supply in a full-scale waste-rock pile. Vadose Zone Journal, **17**(1):1–14. doi:10.2136/vzj2018.06.0119.

Vriens, B., Peterson, H., Laurenzi, L., Smith, L., Aranda, C., Mayer, K.U., and Beckie, R.D. 2019. Long-term monitoring of waste-rock weathering at the Antamina mine. Chemosphere, **215**: 858–869. doi:10.1016/j.chemosphere.2018.10.105.

Wilson, G.W. 1990. Soil evaporative fluxes for geotechnical engineering problems. University of Saskatchewan.

Yanful, E.K., Mousavi, S.M., and Yang, M. 2003. Modeling and measurement of evaporation in moisture-retaining soil covers. Advances in Environmental Research, **7**(4): 783–801. doi:10.1016/S1093-0191(02)00053-9.

Yazdani, J., Barbour, L., and Wilson, W. 2000. Soil water characteristic curve for mine waste rock containing coarse material. In Proceedings of the Canadian Society of Civil Engineers (CSCE) Annual Conference, London, Ont(pp. 7–10).